Enhanced activation of ultrasonic pre-treated softwood biochar for efficient heavy metal removal from water

Aneeshma Peter[a], Bruno Chabot[a], Eric Loranger[a*]

[a] I2E3 – Institut d'Innovations en Écomatériaux, Écoproduits et Écoénergies, à base de biomasse, Université du Québec à Trois-Rivières, 3351, boul. des Forges,

Trois-Rivières, Québec, Canada G8Z 4M3

* Corresponding author:

Tel: +1 819 376-5011, poste 4518

Fax: +1 819 376-5148

E-mail: Eric.Loranger1@uqtr.ca

Abstract

Physical and chemical modification on biochar is an interesting approach to enhance the properties and make them potential candidates in adsorption of heavy metals from water. Studies have shown that ultrasound treatments as well as alkali activations on biochar has positive impact on adsorption behaviour of the material. Base activation on biochar derived from ultrasound pre-treated woodchips were studied to understand the influence of ultrasound pre-treatment on chemical modification of biochar and the adsorption properties emerged from it. 40 and 170 kHz ultrasound pre-treated softwood woodchips were subjected to laboratory scale pyrolysis and the resulted biochars were treated with NaOH. The physicochemical properties were examined, and the adsorption experiments revealed that ultrasound pre-treatment assisted biochars have better adsorption capacity as compared to untreated biochar samples after activation. 170 kHz pre-treated sample exhibited an equilibrium adsorption

capacity of 19.99 mg/g which is almost 22 times higher than that of corresponding non-activated sample. The ultrasound pre-treated samples showed improved competitive adsorption behaviour towards copper ions in comparison with nickel or lead. The overall study suggests that ultrasound pre-treated biochars combined with alkali activation enhances the heavy metal removal efficiency and these engineered biochars can be used as an effective adsorbent in the field of wastewater treatment.

Keywords: Biochar, softwood chips, ultrasound pre-treatments, base activation, adsorption properties, heavy metal removal

1. Introduction

Fresh water contamination prevailing due to non-biodegradable pollutants have been an alarming issue during the past few decades. Rapid industrialization, urbanization, energy generation, improper waste management and other anthropogenic sources have been significantly contributed towards the environmental and health risks arising from these contaminants (Masindi and Muedi, 2018; Inyang et al., 2016). Heavy metals subsidizing a major share have grown high concern due to their reluctance and persistence in the environment and their ability to enter food chain through bioaccumulation. Severe health hazards associated with these toxic metals require the development of effective methodologies to remove them from industrial effluents, thereby ensure sustainability of water resources and control the toxic impacts on living organisms (Barakat, 2011). Electrocoagulation, membrane filtration, and precipitation are few among them. However, higher operational cost, lower selectivity, complex processability and production of hazardous by-products made them less effective in large-scale applications (Ince and Ince, 2017).

Design flexibility and regenerability of adsorbent materials have promoted adsorption as an economic and effective method for heavy metal removal. Among them, activated carbons (AC)

are most predominant due to their ability in wastewater treatment and eco-friendly nature. Nevertheless, depletion in natural reserves of coal, one of the primary sources for AC, has steeply increased the price of this material. They also lack exchange capacity depending on the synthesis routes used, which is an important physicochemical property for the removal of heavy metals (Mohan and Pittman Jr, 2007).

In recent years, biochar has motivated many researchers due to its multi-functionality and effective properties compared to charcoal or other activated carbon materials. Proper specific surface area, porosity and availability of surface functional groups etc makes them a better alternative to other carbon materials for adsorption. Adsorption of various heavy metals like aluminium, arsenic, cadmium, chromium, copper, lead, mercury, nickel, uranium, and zinc are well studied using biochar as adsorbent (Tan et al., 2015; Mohan et al., 2014). A proper understanding of the physicochemical characteristics of biochar and its structure-property relationship towards the heavy metal removal can aid to develop new methodology with enhanced adsorption properties.

Activation is the important technique to improve adsorption efficiency through modification of the surface morphology by increasing the specific surface area and porosity. Physical and chemical activations are mostly used to enhance the adsorption behaviour of materials like biochar (Sajjadi et al., 2019; Angin et al., 2013). Physical activation makes use of high temperature techniques involving steam, CO_2 or other gaseous forms or mechanical forces like ultrasonication to modify the structure of material. The latter technique involves the impregnation of acid or base onto the carbon materials thereby modifying the surface morphology. Chemical activation is normally preferred over physical activation because of high yield, lower temperatures and short activation time compared to other techniques. The mechanism of chemical activation is not well understood, though it assumes that the chemical activation agent forms a cluster of micro- and meso- pores that significantly enhance the

surface area and activates oxygen-rich surface functional groups (Prapagdee et al., 2016). Studies suggest that physical mixing of wood biochar with NaOH increases the specific surface area and adsorption capacity of pharmaceutical compounds from aqueous solution (Taheran et al., 2016). Li et al. (2017) observed that Cd sorption capacity of NaOH activated rape straw biochar was 92% greater as compared to untreated biochar. Economically feasible and effective activation methods are recommended in this perspective, thereby improving the material efficiency.

Very few reports were encountered on investigating ultrasound assisted chemical modification of biochar. Chattergee et al. (2018) has shown that ultrasound-intensified amination enhances the CO_2 capture capacity of biochar derived from pinewood. Similarly, a study by Sajjadi et al (2019) demonstrated that functionalisation of low frequency modified biochar using urea has positively affected metal adsorption capacities of pine wood biochar. Recently, we have seen that ultrasonic pre-treatment influences the adsorption behaviour of softwood-derived biochar with an enhancement of equilibrium adsorption under low frequency exposure (Peter et al., 2020). The 40 kHz pre-treated samples exhibited maximum of 52 percent increase in equilibrium adsorption capacity (Q_e) when compared with untreated biochars. Adsorption characteristics were dependent on the frequency in combination with power versus time and temperature of ultrasound. Detailed investigation on kinetic, isotherm and thermodynamic models showed that the mechanical effect of ultrasound plays a vital role in enhancing the surface. However, mechanism behind high and low frequency pre-treated samples were different from each other, which motivated us to explore the pre-treatment assisted activation on these biochar samples.

Herein, we are evaluating the effect of ultrasound pre-treatments towards the base activation process in biochar and thereby influencing the metal adsorption behaviour of the materials. Due to the heterogeneity and feedstock dependency for physicochemical properties, mix-wood

4

chips are rarely used for adsorption studies, therefore comparable studies available for activation and adsorption using biochar derived from mixed softwood is limited (Chen et al., 2011; Shen et al., 2018; Tomczyk et al., 2020). To the best of our knowledge, this is the first ever study focusing on the effect of combination of alkali activation towards power ultrasound pre-treated mix-wood biochar and study its heavy metal removal efficiency from water. This study focuses on potential application of biochar from sustainable resources like biomass, and validating methodologies to improve its efficiency. Efficient large-scale use of these biochars will be a significant footstep in the field of emerging materials for environmental protection.

2. Materials & Methods

2.1 Biochar production

The biochar used in this study were produced from mix of softwood, which are post-consumer feedstocks from a local Canadian pulp and paper mill. The wood chips (5 mm by 5 mm sized needles) were processed under different ultrasonic pre-treatment conditions as discussed in our previous publications. (Peter et al., 2020; Peter et al., 2019). It was seen that the combination of power, time and bath temperature equally contributed towards adsorption capacities of the material. Hence, the maximum and minimum pre-treatment conditions were used in this work (Table 1) to investigate the pre-treatment effect on activation of biochar. The pre-treated woodchips were dried in an oven at 105 °C for at least 48 h before being used in the pyrolysis reactor. Slow pyrolysis was performed in a laboratory-scale set up as reported previously by Loranger et al (2016). Each pyrolysis was performed three times to confirm consistency and the products were collected separately. The resulting biochar was subjected to alkali activation. The physicochemical characteristics of biochar were studied before and after base-activation.

Table 1. List of ultrasound pre-treatments on woodchips

Sample Code	Frequency	Power	Temperature	Time
	(kHz)	(W)	(°C)	(h)
Act-Untreated	-	-	-	-
Act-UST1	40	1000	80	2
Act-UST2	40	250	20	1
Act-UST3	170	1000	80	2
Act-UST4	170	250	20	1

2.2 Base activation of as-synthesized biochar

The alkali modification was done as previously reported by Taheran et al. (2016). About 10 g of NaOH was dissolved in 50 mL of water and 5 g of biochar was added to it. The mixture was stirred at room temperature for 3 h, filtered and dried at 105 °C for 24 h. This sample was placed in a quartz-tube furnace under argon flow. The temperature was increased to 800 °C at 10 °C/min and held at this temperature for 2 h before cooling down to room temperature. Then, the product was washed with water and the NaOH was neutralized with 0.1 M HCl. Inorganic-by-product was removed by water wash and the resulting product was dried at 60 °C for 24 h. Base activated samples, pre-treated with ultrasounds, are identified as Act-UST throughout the study.

2.3 Characterisation of biochar

About 1:10 weight by volume biochar and deionized water ratio were stirred at room temperature for 2 h. The pH of the sample was measured using Accumet XL20, Thermo Fisher Scientific pH-meter and the surface zeta potential (mV) was measured with Zetasizer-nano series from Malvern Instruments. The reflection mode infrared spectra were recorded in Nicolet

iS10 Smart iTR Infrared Spectroscopy instrument using KBr pellet in the range of 400-4000 cm^{-1} for a minimum of 16 scans with 1 cm^{-1} resolution. The surface morphology of the biochar was studied using Scanning Electron Microscopy (SEM) images captured using Hitachi SU1510 instrument. Energy Dispersive X-ray Spectroscopy (EDX) was obtained with X-Max, Oxford instrument to verify the surface carbon and oxygen content. Surface area was measured using the Brunauer, Emmett and Teller (BET) method that measures N_2 gas sorption (0.162 nm^2) at 77 K. Approximately 100 mg of biochar was outgassed at 200 °C for 16 h and then analysed on an Autosorb-1 Surface Area Analyzer by Quantachrome Instruments.

2.4 Adsorption experiments

The metal adsorption behaviour of biochar was studied using batch adsorption technique with Copper as model metal contaminant. 1000 ppm stock solution of Cu (II) was prepared by dissolving analytical grade anhydrous $CuSO_4$ in deionized water. The pH of salt solution was maintained at 5 to avoid salt precipitation at higher pH. In a 125 mL Erlenmeyer flask, 5 g/L biochar was added to 100 ppm Cu (II) solution and agitated on a reciprocating shaker at room temperature (22 ± 2 °C) at 150 rpm. For the kinetic experiments, samples were taken at specific time intervals and immediately filtered using Whatman No. 1 filter paper. The residual heavy metal concentration in the filtrate was measured using EDTA titration described by Prasad and Raheem, (1993). The amount of adsorbed metal ions, Q (mg/g), was calculated using Eq. (1).

$$Q \left(\frac{mg}{g}\right) = \frac{(C_{initial} - C_{final}) ppm * V(L)}{m\ (g)} \tag{1}$$

The experimental data was fitted to nonlinear forms of Pseudo First and Pseudo Second order kinetic models using Eq. (2) and (3), respectively.

$$Q_t = Q_e * (1 - e^{-k_1 t}) \tag{2}$$

$$Q_t = \frac{Q_e^2 * k_2 * t}{1 + Q_e * k_2 * t} \tag{3}$$

Where Q_t and Q_e (mg/g) are adsorbed metal amount at time t (min) and equilibrium, k_1 and k_2 are the rate constants for pseudo first order and second order kinetic model, respectively.

Most common isotherm models for biochar adsorption, Freundlich and Langmuir were examined with initial Cu (II) concentrations ranging from 10 to 100 ppm using nonlinear regression with Eq. (4) and (5), respectively.

$$Q_e = K_f * C_e^{1/n} \qquad (4)$$

$$Q_e = \frac{Q_{max} * b * C_e}{1 + b * C_e} \qquad (5)$$

Where Q_e is the amount of the metal adsorbed at equilibrium (mg/g), C_e is the equilibrium concentration of solution (mg/L). K_f and n are indicators of adsorption capacity and intensity, respectively. Q_{max} is the maximum adsorption capacity (mg/g) and b is related to degree of adsorption affinity of the adsorbate.

The temperature effect was assessed at temperatures 25, 40, and 60 ^{o}C and the thermodynamic parameters were calculated as explained in literatures (Al-Anber, 2011; Batool et al., 2018).

2.5 Multicomponent adsorption

Isotherm experiments were carried out at room temperature by adding 5 g/L biochar to 125 mL Erlenmeyer flask containing tertiary metal (Pb^{2+}, Cu^{2+} and Ni^{2+}) solutions of Pb $(NO_3)_2$, anhydrous $CuSO_4$ and Ni $(NO_3)_2.6H_2O$. The concentration of Cu (II) and Ni (II) ions were ranged from 10 ppm to around 80 ppm in the initial mixed metal solution. However, at higher concentration Pb (II) started to precipitate resulting in lower concentration in the mixed solution. Therefore, the initial concentration of Pb (II) was ranged from 10 ppm to around 40 ppm in the tertiary metal system. Initial pH of the metal solutions was adjusted to about 5.0 using 0.1 M HCl and 0.1 M NaOH to avoid precipitation. The mixture was shaken for 3 h in a rotary shaker to ensure the equilibrium was reached and filtered using Whatman 1 filter paper.

Concentrations of Pb^{2+}, Cu^{2+} and Ni^{2+} in the filtrate were determined using MP–AES (4210 Agilent CrossLab, USA). The adsorption capacities were calculated using Eq (1).

2.6 Statistical regression for experimental data

All the adsorption experiments were performed three times to ensure consistency and the mean values reported with standard error in experimental plots. Experimental data were fitted with non-linear forms of equation using OriginPro software (version 9.6).

3. Results and Discussion

3.1 Effect of alkali activation after ultrasound pre-treatment on surface morphology and chemical properties of biochar

Scanning Electron Microscope images were captured and examined to understand the pre-treatment induced activation effects on surface morphology (Fig. 1). From common knowledge, the surface was significantly ruptured and microchannels and pits were more open after activation. These topology changes were more obvious in ultrasound pre-treated samples with a fully developed porous structure and increased heterogeneity on surface. The change in surface morphology is a positive implication since this could influence the adsorption characteristics of the material, especially after activation.

(a)　　　　　　　　　　(b)

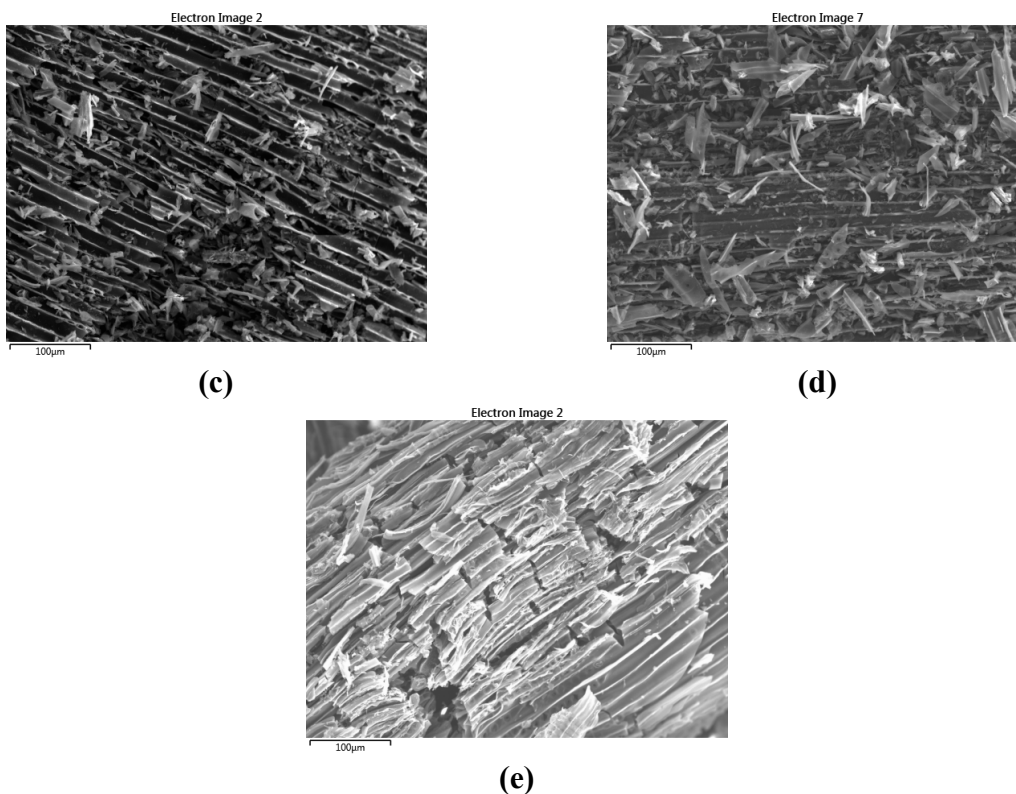(c)   (d)

(e)
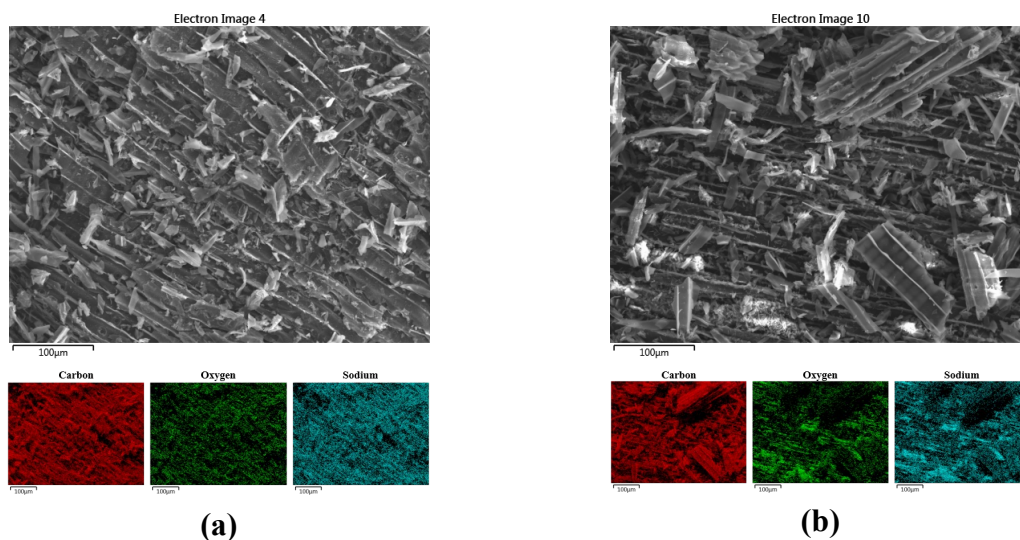
Fig. 1. Scanning electron Microscope images with EDX mapping of (a) Act-UST1 (40 kHz, 1000 W at 80 °C for 2 h) (b) Act-UST3 (170 kHz, 1000 W at 80 °C for 2 h) and Scanning electron microscope images of (c) Act-UST2 (40 kHz, 250 W at 20 °C for 1 h) (d) Act-UST4 (170 kHz, 250 W at 20 °C for 1 h) and (e) Act-Untreated at magnification at 250x magnification

To identify the elements present on the surface, the activated biochar samples were scanned using EDX analyser and compared with corresponding as-synthesized samples. EDX give an understanding about relative atomic percent distribution on the surface for a better comparison (Fig. S1-S5). Results expressed in Table 2 excludes the count of hydrogen on the biochar surface. The major atomic percentage on surface is carbon which ranges from 81 to 87 atomic percentage compared to other elements. Almost 10 percent oxygen content in all samples could be the result of oxygen containing surface functional groups on the surface.

Table 2. Surface characteristics of biochar after base activation

Sample	pH	Zeta potential (mV)	C At%	O At%	Na At%
Act-Untreated	5.4	-13.87	85.2	11.6	3.2
Act-UST1	6.3	-9.45	81.3	13.3	5.4
Act-UST2	6.4	-6.57	85.6	10.7	3.7
Act-UST3	5.3	-2.99	78.6	16.8	4.4
Act-UST4	5.3	-9.37	87.1	10.3	2.6

It was interesting to note that a significant atomic percent of sodium on the activated biochar surface were present even after thorough washing with water to remove salt. Act-UST1 and Act-UST3 has a relatively larger atomic percent of oxygen, and hence larger amount of Na compared to others. The EDX mapping results show that these sodium ions are present almost at the same position as oxygen (Fig. 1). Na$^+$ ions could be electrostatically bonded with the remaining oxygen present on the carbon surface which was reluctant even after activation. From the image, it is clear that these sodium ions are homogenously distributed over the surface. This is a good indication that the synthesized biochar could provide cation exchange ability, hence they can effectively replace exchangeable metal ions on the surface.

Surface charge plays important role in adsorption behaviour of biochar, especially in case of charged metal ions as contaminants. In Table 2 the pH and Zeta potential of biochar samples in Cu (II) solution are indicated. The pH of metal solution has increased marginally after adding biochars into it, which shows that the nature of biochars are slightly alkaline. 40 kHz pre-treated samples Act-UST1 and Act-UST2 were found to be more alkaline compared to others. The negative zeta potential of these materials confirms that the surface is negatively charged

which could potentially supply adsorption sites for positively charged contaminants on to the surface. The functional groups available for different ionic interactions keeps the biochar surface charged, and they could be mainly oxygen containing functionalities, which are reluctant towards high temperature degradation during pyrolysis. However, the activation process might further remove some of these functionalities during heating, yet the surface remained negatively charged. The ultrasound pre-treated samples were slightly less negative compared to control sample (Act-Untreated), nevertheless Act-UST3 was less negatively charged amongst all.

Maximum carbonization of NaOH treated biochar was confirmed by examining FT-IR spectra (Fig 2, FT-IR spectra of all activated samples were identical). No significant bands were observed in higher wavelength region, indicating that most of the aliphatic chains are removed from surface and most condensed aromatic structure. However, aromatic region shows low intensity bands at 1300 cm^{-1} corresponding to C-O, COO$^-$ asymmetric stretches, which is a clear indication that a substantial amount of oxygen containing functionalities are still available for ionic interactions.

3.2 Influence of ultrasound pre-treatment assisted activation on adsorption properties

The effect of contact time on adsorption capacity of the material is an interesting parameter to investigate in order to understand the nature of kinetic behaviour of the material. As seen in Fig. 2, the Cu (II) uptake on biochar samples were very fast with a saturation time of approximately 30 min. The equilibrium was achieved within 1 min for Act-Untreated and 40 kHz pre-treated samples (Act-UST1 and Act-UST2). In the case of 170 kHz samples, almost 90 percent of adsorption happened slowly during the first 15 min and then achieved equilibrium over 1 h.
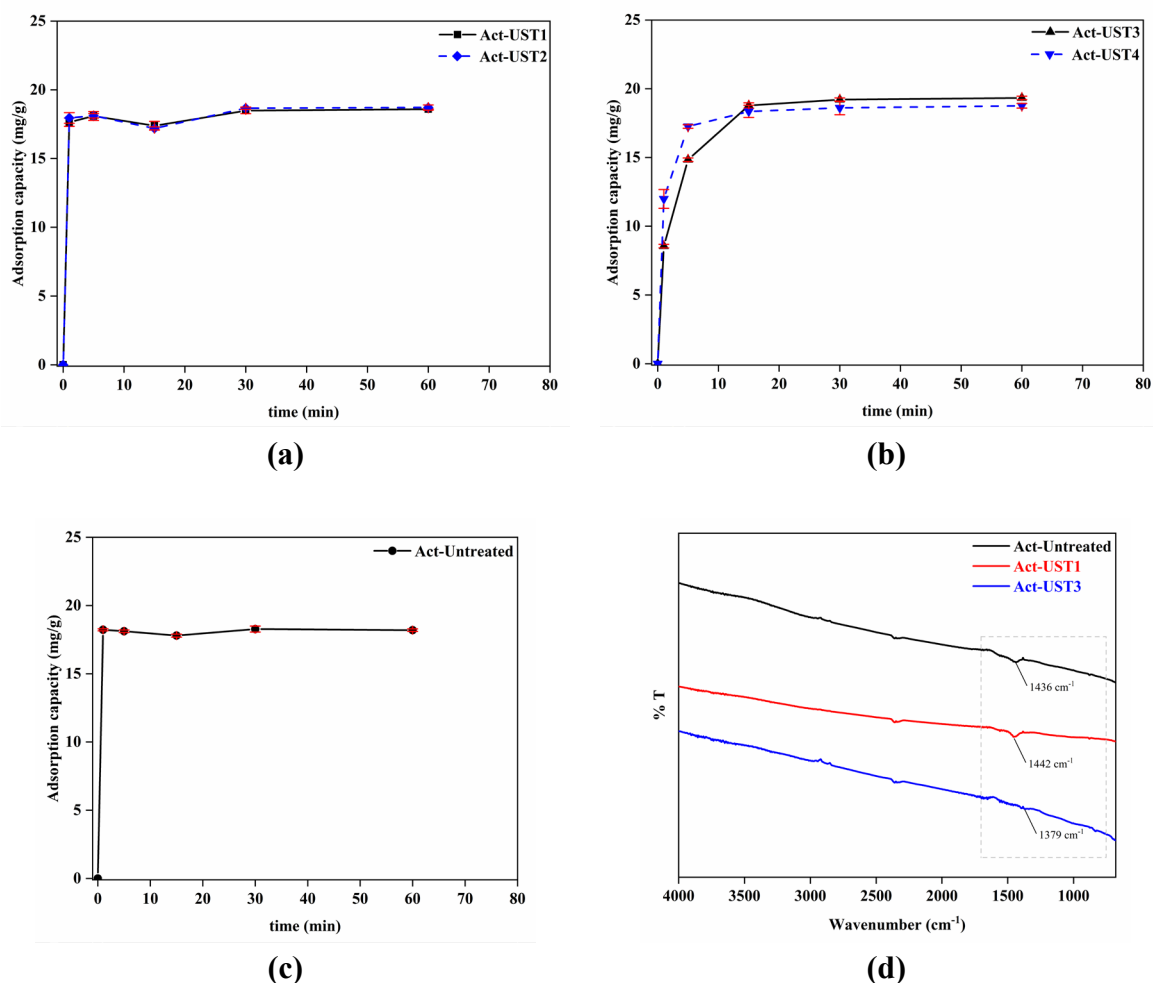
Fig. 2. Effect of contact time on adsorption capacity of biochar samples (a) Activated biochar with 40 kHz ultrasound pre-treatment (b) Activated biochar with 170 kHz ultrasound pre-treatment and (c) Activated biochar without ultrasound pre-treatment and (d) FTIR comparison of Act-Untreated, Act-UST1 and Act-UST3 to confirm maximum carbonization.

In most of the case, the mechanism of heavy metal adsorption on biochars are explained using pseudo first order and pseudo second order kinetic equations. Pseudo first order kinetics did not apply to the complete range of the contact time; therefore, the calculations were omitted. This could be possible because pseudo first order reactions depend on the concentration of both adsorbate and adsorbent and one of the components is present in large excess. They are generally classified as physisorption where adsorption rate depends on the number of available adsorption sites. Therefore, its concentration changes very slowly as the contact time increases, whereas in our case there is a rapid change in concentration of adsorbate and quick saturation

on heterogenous adsorption sites (Li et al., 1999; Rudzinski and Plazinski, 2006; Lee et al., 2011). Nevertheless, pseudo second order kinetics fitted well with the experimental data, with $R^2 > 0.9934$. This elucidates chemisorption as the rate limiting mechanism, mostly ion exchange interactions which are generally rapid reactions (Shen et al. 2018). The results represented in Table 3 shows that ultrasound pre-treated biochars have higher equilibrium adsorption capacity (Q_e) after activation, when compared with ultrasound untreated sample. 170 kHz pre-treated samples were better with adsorption capacity in comparison with 40 kHz samples. Among them, Act-UST3 exhibited highest Q_e. However, the kinetic rate was decreased with ultrasound pre-treatments, interestingly lowest k was observed in Act-UST3 and Act- Untreated showed fastest kinetics with k value of 7.88 g/mg.min. This suggests that ultrasound pre-treatment enhances the activation process and thereby improves the adsorption capacity of material with higher frequency has better impacts on equilibrium adsorption capacity. Nevertheless, the rate of adsorption decreases upon ultrasonic pre-treatments. At higher frequency, a greater number of impulsive cavitation bubbles intensify the opening of existing pores of biochar, thereby increases the permeability of guest molecules into these pores. As shown by Q_e values of different pre-treated biochars (Table 3), the combination of higher frequency, power, bath temperature and time exhibited better adsorption when compared to other pre-treatments. This effect was marginal at lower frequency and power combinations yet showed better adsorption capacity than the untreated one. These results demonstrate that the ultrasonic pre-treatments affect both physical and chemical characteristics of the synthesized biochars.

Table 3. Parameters of Pseudo second order kinetic models for Cu (II) adsorption on biochar samples

Sample	Pseudo Second order kinetic parameters		
	Q_e	k	R^2
	(mg/g)	(g/mg. min)	
Act-Untreated	18.12	7.88	0.9993
Act-UST1	18.19	1.67	0.9961
Act-UST2	18.20	3.23	0.9934
Act-UST3	19.99	0.03	0.9962
Act-UST4	19.03	0.09	0.9997

It was clearly demonstrated that ultrasound pre-treatments have positive impact on base activation, hence the equilibrium adsorption capacities of the samples were improved. To evaluate how prominent these enhancements are, the Q_e (mg/g) and BET-N_2 specific surface area of synthesized samples were compared with a commercially available activated carbon samples (Fluval) along with few of the reported wood biochars from literature (Table 4). The equilibrium adsorption capacities of Act-UST1 and Act-UST3 are considerably good among the wood biochars reported previously and almost 12 and 22 times higher than non-activated UST samples, respectively. The specific surface area was also significantly increased after activation. Ultrasound pre-treatments help the activation to develop improved porous structure and thereby increasing the specific surface area of the material. The sono-chemical effect was dominant in this case resulting in better BET surface area of Act-UST3 (170 kHz) than Act-UST1 (40 kHz). Regardless of the higher specific surface area of activated carbon, our samples exhibited better adsorption capacity after base activation as shown in Table 3. The enhanced

surface area along with surface functionalities facilitated the anchoring of guest contaminants towards the surface thus, resulted in better adsorption capacity of the biochars. The ultrasonic pre-treatments enhance the mass and heat transfer during various interactions, and it helps to increase the NaOH interaction with surface functionalities during alkali modification. At higher frequency and power, this effect could be considerably enhanced because of the larger number of cavitation bubbles and microjet impulsions associated with it.

Table 4. Comparison of BET surface area and copper adsorption capacities of wood-derived biochars from literature

Feedstock	Activation Method	BET Surface Area (m^2/g)	Adsorption Capacity (mg/g)	Reference
Pine wood	Hydrothermal	21	4.21	Liu et al., 2010
Pinewood	-	29	2.73	Liu et al., 2010
Hard wood	-	0.43	6.49	Chen et al., 2011
Softwood	Steam	383.66	0.476 (mmol/g)	Han et al., 2013
Hardwood	Steam	343.91	0.307 (mmol/g)	Han et al., 2013
Hickory wood	$KMnO_4$	205	14.45	Wang et al., 2015
Hickory wood	-	101	7.6	Wang et al., 2015
Jarrah	-	309.29	4.39	Jiang et al., 2016
Pinewood	-	219.35	1.47	Jiang et al., 2016
Mix wood	-	26.40	0.019 (mmol/g)	Shen et al., 2018
Wood waste	-	83.6	2.9	Tomczyk et al., 2020
Willow wood	-	-	4.09	Wang et al., 2020
AC (Fluval)	-	718.42	4.62	Peter et al., 2020

UST1	40 kHz UST	12.4	1.54	Peter et al., 2020
UST3	170 kHz UST	3.31	0.92	Peter et al., 2020
Act-UST1	40 kHz UST + NaOH	**368.63**	**18.19**	This study
Act-UST3	170 kHz UST + NaOH	**503.60**	**19.99**	This study

The initial metal concentration was linearly related to adsorption capacity of the material (Fig. S6) which shows that the adsorption capacity of the material increases with the number active sites available for different interactions. To better understand adsorbent-adsorbate interactions, most frequently used adsorption isotherm models Langmuir and Freundlich were applied on to the experimental data. With respect to the linear regression coefficient R^2, the adsorption of metal ions onto biochar was better described by Freundlich isotherm model, suggesting multilayer adsorption on a heterogenous surface (Table 5). The surface heterogeneity constant n values were slightly higher for Act-UST samples, indicating that the isotherms changed from linear to strong nonlinear with ultrasonic pre-treatments. The highest n value for Act-UST3 indicates more heterogeneous surface. The value for K_f which is related to maximum adsorption capacity was highest for Act-UST3. Better K_f values of UST biochars further indicates that the adsorption followed by ultrasound pre-treated samples are better than the untreated biochar. The intensive support of ultrasound pre-treatments for better opening of channeled pores and larger specific surface along with the grafting of active sites using NaOH, substantially improved the adsorbent-adsorbate interactions which leads to better adsorption behaviour of the materials.

Thermodynamic parameters such as change in enthalpy ΔH^0 and entropy ΔS^0 as well as Gibb's free energy ΔG^0 were calculated in order to determine the thermodynamically favourable

conditions for adsorption (Table 5). The positive value of ΔH^0 for all biochar samples revealed that the adsorption is endothermic, which is similar to most of the previous studies on biochar adsorption (Chen et al., 2011; Kołodyńska et al., 2012; Van Vinh et al., 2015). The increase in temperature provides enough energy for metal ions to be captured onto the interior structure of biochar. The change in enthalpy, and therefore, the degree of randomness ΔS^0 is less for high frequency pre-treated samples. This indicates that the structural changes occurred in these samples are lower compared to others during adsorption.

Table 5. Freundlich isotherm and thermodynamic parameters of biochar samples

Sample	Freundlich Model			Temperature	Thermodynamic parameters		
	K_f	n	R^2	(K)	ΔG^0 (kJ/mol)	ΔH^0 (kJ/mol)	ΔS^0 (J/mol K)
Act-Untreated	0.096	0.88	0.9999	295	-1.75	14.77	56.00
				313	-2.76		
				333	-3.88		
Act-UST1	0.103	0.89	0.9998	295	-1.71	14.30	54.28
				313	-2.68		
				33	-3.77		
Act-UST2	0.127	0.93	0.9990	295	-1.52	20.48	74.58
				313	-2.86		
				333	-4.35		
Act-UST3	0.129	0.93	0.9997	295	-1.62	11.48	44.40
				313	-2.41		
				333	-3.30		

Act-UST4	0.108	0.90	0.9990	295	-1.90	6.81	29.54
				313	-2.43		
				333	-3.03		

The negative value of Gibb's free energy ΔG^0 indicates that the adsorption is spontaneous, hence the adsorption and desorption is in thermal equilibrium. The system is more spontaneous when external energy is provided. These values were almost similar with all samples, however, high frequency pre-treated samples showed comparatively lower ΔG^0 value, which was also the case of ΔS^0. Overall, it is obvious that the high frequency samples are exhibiting a different thermodynamic behaviour compared to control or low frequency samples, which could be because of the change in surface behaviour due to the two-step activation of synthesized biochars.

The alkali activated biochars exhibited difference in adsorption properties with respect to the changes in ultrasound pre-treatment conditions. The surface properties and adsorption capacities were remarkable. These engineered biochars can be an efficient cost-effective replacement for activated carbons for heavy metal removal from contaminated water.

3.3 Selectivity of heavy metals on modified biochars

For a more precise understanding on heavy metal selectivity and competitive adsorption of the material, multi metal solutions were analysed. This could give a better assessment on efficiency of the biochars in industrial wastewater recycling processes. The competitive adsorption of metals was different for ultrasound pre-treated and untreated samples. However, among the Act-UST samples, 170 kHz samples displayed effect towards heavy metal uptake. The detailed result is given in Table S1 and shown in Fig.3.
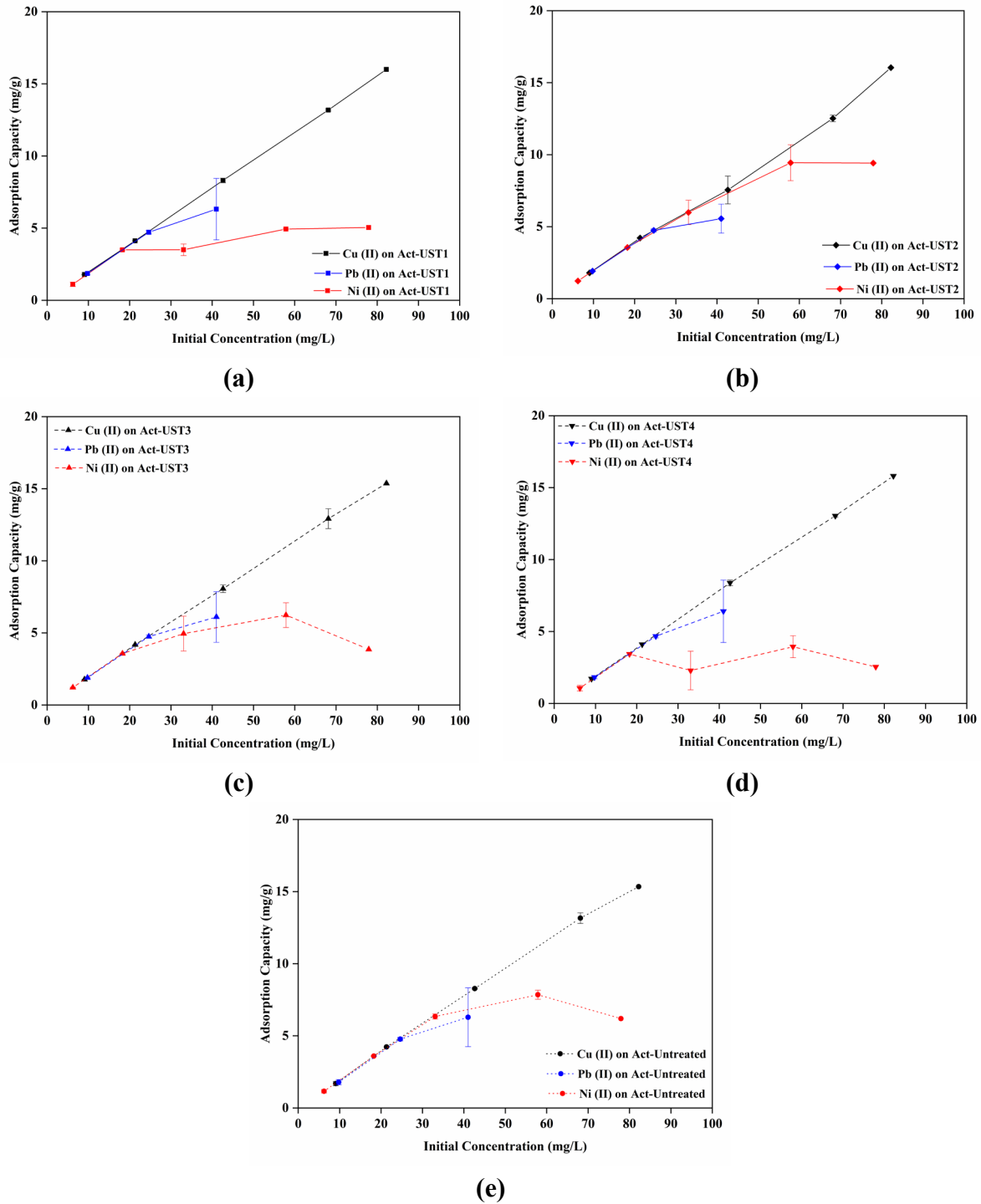
(a)

(b)

(c)

(d)

(e)

Fig. 3. Comparison of competitive metal adsorption for Cu (II), Pb (II) and Ni (II) on to (a) Act-UST1 (40 kHz, 1000 W at 80 $^{\circ}$C for 2 h) (b) Act-UST2 (40 kHz, 250 W at 20 $^{\circ}$C for 1 h) (c) Act-UST3 (170 kHz, 1000 W at 80 $^{\circ}$C for 2 h) (d) Act-UST4 (170 kHz, 250 W at 20 $^{\circ}$C for 1 h) and (e) Act-Untreated

As represented in Fig. 3, the competitive adsorption capacity of biochar towards copper increased linearly with increase in initial concentration. However, in the case of Ni (II) and Pb (II) it did not follow the linear relation. At higher concentrations, all samples exhibited selective adsorption of Cu (II) over other two metals, with ultrasound pre-treated samples displayed a small improvement in adsorption capacity than untreated sample. On the other hand, the copper adsorption capacity of Act-UST3 at 100 ppm was reduced by approximately 20 percent as compared to single component system. A similar trend was observed by Mahdi et al. (2019) in their study with competitive adsorption of Pb (II), Cu (II) and Ni (II) ions on date seed biochars. Because of the similar ionic size of Cu (II) and Ni (II) when compared to Pb (II), their competitiveness was expected to be same onto biochars. However, despite of the higher selectivity towards copper ions, Act-UST1, Act-UST-3 and Act-UST4 exhibited better adsorption for lead over nickel. Besides, it was interesting to note that Act-Untreated and Act-UST2 behaved similar towards competitive uptake of all three ions, particularly nickel preferred over lead. This justifies that low power and frequency ultrasound does not influences the surface openings of the biochar much, which further resulted in less adsorption capacity of bigger ions in the mixed solution.

4. Conclusion

In this study we have seen that alkali activation of ultrasound pre-treated softwood biochar has improved physical as well as metal adsorption properties. Higher frequency ultrasound enhances the activation process, thus modifies surface of the biochar favouring the metal adsorption capacity. The ultrasound pre-treatment facilitated the accessibility of a heterogenous surface with wide opening of already existing pores and microchannels, and the alkali treatment improved the availability surface anchoring sites. The underlying mechanism was found to be chemisorption, expected to be ion exchange reactions resulting from the sodium ions present on the surface anchoring sites. The higher equilibrium adsorption

capacities of Act-UST samples in comparison with other reported wood biochars show that the synthesized biochars can be an efficient candidate for heavy metal removal from wastewater. Isotherm and thermodynamic studies also suggest that the Act-UST samples have improved physicochemical properties. The better adsorption properties of ultrasound pre-treated biochars, especially higher frequency pre-treated samples showed that combination of frequency, power, temperature and exposure time influences the base modification on the material. The two-step activation of the biochars exhibited promising adsorption capacities in the mixed metal systems as well. The higher selectivity towards copper ions indicates that these materials can be potentially used to remove particular ions from a mix of metal-contaminated solution. This study encourages to make use of power ultrasound enhanced modifications on biochar with better physicochemical properties and aides the potential conversion of feedstock residues towards process control and design.

Acknowledgement

References

Al-Anber MA. Thermodynamics approach in the adsorption of heavy metals: INTECH Open Access Publisher, 2011. https://doi.org/10.5772/21326

Angın D, Köse TE, Selengil U. Production and characterization of activated carbon prepared from safflower seed cake biochar and its ability to absorb reactive dyestuff. Appl. Surf. Sci. 2013; 280: 705-710. https://doi.org/10.1016/j.apsusc.2013.05.046

Barakat M. New trends in removing heavy metals from industrial wastewater. Arab. J Chem. 2011; 4: 361-377. https://doi.org/10.1016/j.arabjc.2010.07.019

Batool F, Akbar J, Iqbal S, Noreen S, Bukhari SNA. Study of isothermal, kinetic, and thermodynamic parameters for adsorption of cadmium: an overview of linear and nonlinear approach and error analysis. Bioinorganic chemistry and applications 2018; 2018. https://doi.org/10.1155/2018/3463724

Chatterjee R, Sajjadi B, Mattern DL, Chen W-Y, Zubatiuk T, Leszczynska D. Ultrasound cavitation intensified amine functionalization: A feasible strategy for enhancing CO_2 capture capacity of biochar. Fuel 2018; 225: 287-298. https://doi.org/10.1016/j.fuel.2018.03.145

Chen X, Chen G, Chen L, Chen Y, Lehmann J, McBride MB. Adsorption of copper and zinc by biochars produced from pyrolysis of hardwood and corn straw in aqueous solution. Bioresour. Technol. 2011; 102: 8877-8884. https://doi.org/10.1016/j.biortech.2011.06.078

Han Y, Boateng AA, Qi PX, Lima IM, Chang J. Heavy metal and phenol adsorptive properties of biochars from pyrolyzed switchgrass and woody biomass in correlation with surface properties. J. Environ. Manage. 2013; 118: 196-204. https://doi.org/10.1016/j.jenvman.2013.01.001

Ince M, Ince OK. An overview of adsorption technique for heavy metal removal from water/wastewater: A critical review. Int. J. Pure Appl. Sci 2017; 3: 10-19. https://doi.org/10.29132/ijpas.358199

Inyang MI, Gao B, Yao Y, Xue Y, Zimmerman A, Mosa A. A review of biochar as a low-cost adsorbent for aqueous heavy metal removal. Crit. Rev. Environ. Sci. Technol. 2016; 46: 406-433. https://doi.org/10.1080/10643389.2015.1096880

Jiang S, Huang L, Nguyen TA, Ok YS, Rudolph V, Yang H. Copper and zinc adsorption by softwood and hardwood biochars under elevated sulphate-induced salinity and acidic pH conditions. Chemosphere 2016; 142: 64-71. https://doi.org/10.1016/j.chemosphere.2015.06.079

Kołodyńska D, Wnętrzak R, Leahy J, Hayes M, Kwapiński W, Hubicki Z. Kinetic and adsorptive characterization of biochar in metal ions removal. Chem. Eng. J. 2012; 197: 295-305. https://doi.org/10.1016/j.cej.2012.05.025

Lee C-R, Kim H-S, Jang I-H, Im J-H, Park N-G. Pseudo first-order adsorption kinetics of N719 dye on TiO2 surface. ACS applied materials & interfaces 2011; 3: 1953-1957 https://doi.org/10.1021/am2001696

Li B, Yang L, Wang C, Zhang Q, Liu Q, Li Y. Adsorption of Cd (II) from aqueous solutions by rape straw biochar derived from different modification processes. Chemosphere 2017; 175: 332-340. https://doi.org/10.1016/j.chemosphere.2017.02.061

Li PH, Bruce RL, Hobday MD. A pseudo first order rate model for the adsorption of an organic adsorbate in aqueous solution. Journal of Chemical Technology & Biotechnology: International Research in Process, Environmental & Clean Technology 1999; 74: 55-59 https://doi.org/10.1002/(SICI)1097-4660(199901)74:1<55::AID-JCTB984>3.0.CO;2-D

Liu Z, Zhang F-S, Wu J. Characterization and application of chars produced from pinewood pyrolysis and hydrothermal treatment. Fuel 2010; 89: 510-514. https://doi.org/10.1016/j.fuel.2009.08.042

Loranger, É., Pombert, O., Drouadaine, V. Ultrasonic Pre-treatments of Wood Chips used in a conventional pyrolysis and their effect on bio-oil composition and calorimetry. 2016; SAMPE Conference Proceedings.

Mahdi Z, Yu QJ, El Hanandeh A. Competitive adsorption of heavy metal ions (Pb^{2+}, Cu^{2+}, and Ni^{2+}) onto date seed biochar: batch and fixed bed experiments. Sep. Sci. Technol. 2019; 54: 888-901. https://doi.org/10.1080/01496395.2018.1523192

Masindi V, Muedi KL. Environmental contamination by heavy metals. Heavy metals 2018; 10: 115-132. https://doi.org/10.5772/intechopen.76082

Mohan D, Pittman Jr CU. Arsenic removal from water/wastewater using adsorbents—a critical review. J. Hazard. Mater. 2007; 142: 1-53. https://doi.org/10.1016/j.jhazmat.2007.01.006

Mohan D, Sarswat A, Ok YS, Pittman Jr CU. Organic and inorganic contaminants removal from water with biochar, a renewable, low cost and sustainable adsorbent–a critical review. Bioresour. Technol. 2014; 160: 191-202. https://doi.org/10.1016/j.biortech.2014.01.120

Peter A, Chabot B, Loranger E. Enhancing Surface Properties of Softwood Biochar by Ultrasound Assisted Slow Pyrolysis. 2019 IEEE International Ultrasonics Symposium (IUS). IEEE, 2019, pp. 2477-2480. https://doi.org/10.1109/ULTSYM.2019.8925793

Peter A, Chabot B, Loranger E. The influence of ultrasonic pre-treatments on metal adsorption properties of softwood-derived biochar. Bioresour. Technol. Rep. 2020; 11: 100445. https://doi.org/10.1016/j.biteb.2020.100445

Prapagdee S, Piyatiratitivorakul S, Petsom A. Physico-chemical activation on rice husk biochar for enhancing of cadmium removal from aqueous solution. Asian J. Water Environ. Pollut. 2016; 13: 27-34. https://doi.org/10.3233/AJW-160004

Prasad KMK, Raheem S. Evaluation of the quality of colour changes of complexometric indicators in the titration of copper (II) with EDTA by tristimulus colorimetry. Microchimica Acta 1993; 112: 63-69. https://doi.org/10.1007/BF01243322

Rudzinski W, Plazinski W. Kinetics of solute adsorption at solid/solution interfaces: a theoretical development of the empirical pseudo-first and pseudo-second order kinetic rate equations, based on applying the statistical rate theory of interfacial transport. J Phys. Chem. B 2006; 110: 16514-16525 https://doi.org/10.1021/jp061779n

Sajjadi B, Broome JW, Chen WY, Mattern DL, Egiebor NO, Hammer N. Urea functionalization of ultrasound-treated biochar: a feasible strategy for enhancing heavy metal adsorption capacity. Ultrason. Sonochem. 2019a; 51: 20-30. https://doi.org/10.1016/j.ultsonch.2018.09.015

Sajjadi B, Chen W-Y, Egiebor NO. A comprehensive review on physical activation of biochar for energy and environmental applications. Rev. Chem. Eng. 2019b; 35: 735-776. https://doi.org/10.1515/revce-2017-0113

Shen Z, Zhang Y, Jin F, Alessi DS, Zhang Y, Wang F. Comparison of nickel adsorption on biochars produced from mixed softwood and Miscanthus straw. Environmental Science and Pollution Research 2018; 25: 14626-14635. https://doi.org/10.1007/s11356-018-1674-2

Taheran M, Naghdi M, Brar SK, Knystautas EJ, Verma M, Ramirez AA. Adsorption study of environmentally relevant concentrations of chlortetracycline on pinewood biochar. Sci. Total Environ. 2016; 571: 772-777. https://doi.org/10.1016/j.scitotenv.2016.07.050

Tan X, Liu Y, Zeng G, Wang X, Hu X, Gu Y. Application of biochar for the removal of pollutants from aqueous solutions. Chemosphere 2015; 125: 70-85. https://doi.org/10.1016/j.chemosphere.2014.12.058

Tomczyk A, Sokołowska Z, Boguta P. Biomass type effect on biochar surface characteristic and adsorption capacity relative to silver and copper. Fuel 2020; 278: 118168. https://doi.org/10.1016/j.fuel.2020.118168

Van Vinh N, Zafar M, Behera S, Park H-S. Arsenic (III) removal from aqueous solution by raw and zinc-loaded pine cone biochar: equilibrium, kinetics, and thermodynamics studies. International journal of environmental science and technology 2015; 12: 1283-1294. https://doi.org/10.1007/s13762-014-0507-1

Wang H, Gao B, Wang S, Fang J, Xue Y, Yang K. Removal of Pb (II), Cu (II), and Cd (II) from aqueous solutions by biochar derived from KMnO4 treated hickory wood. Bioresour. Technol. 2015; 197: 356-362. https://doi.org/10.1016/j.biortech.2015.08.132

Wang S, Kwak J-H, Islam MS, Naeth MA, El-Din MG, Chang SX. Biochar surface complexation and Ni (II), Cu (II), and Cd (II) adsorption in aqueous solutions depend on feedstock type. Sci. Total Environ. 2020; 712: 136538. https://doi.org/10.1016/j.scitotenv.2020.136538
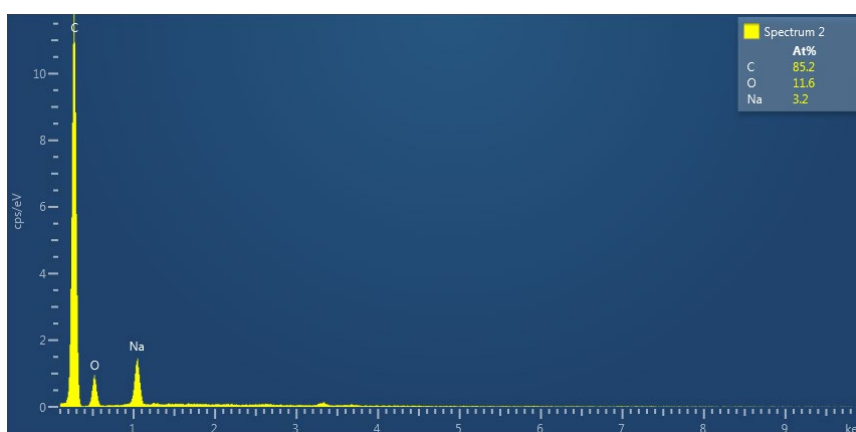
Supplementary Information

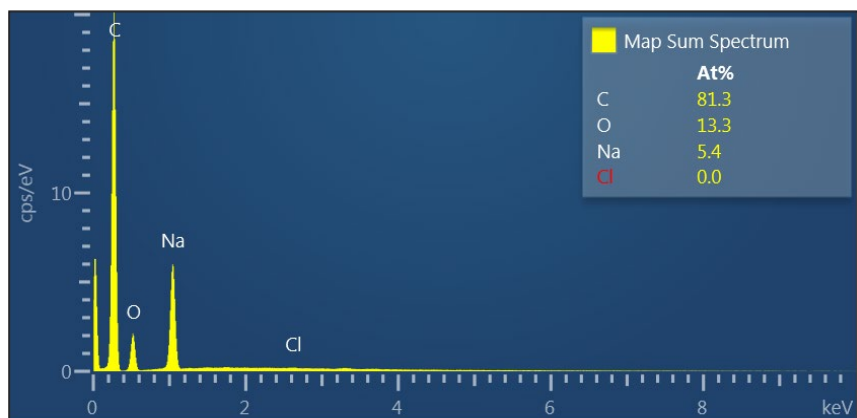Fig. S1. EDX mapping spectra of Act-Untreated

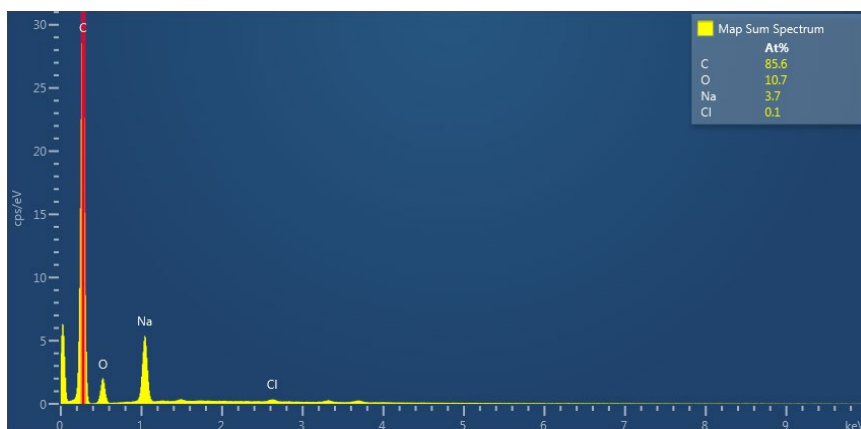Fig. S2. EDX mapping spectra of Act-UST1 (40 kHz, 1000 W at 80 °C for 2 h)

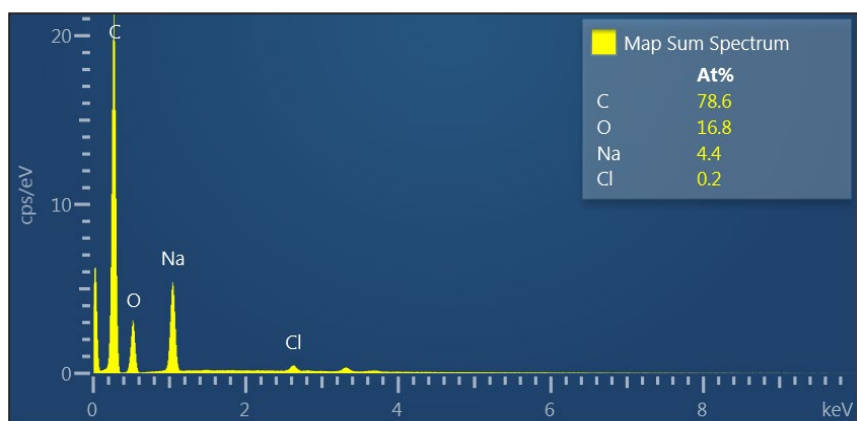Fig. S3. EDX mapping spectra of Act-UST2 (40 kHz, 250 W at 20 °C for 1 h)

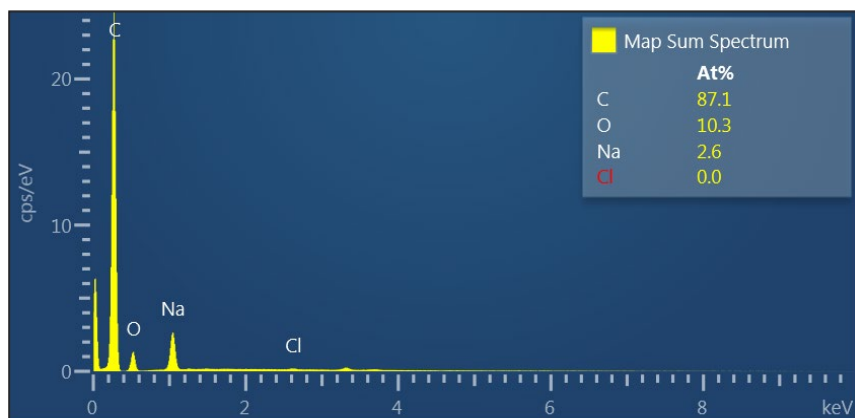Fig. S4. EDX mapping spectra of Act-UST3 (170 kHz, 1000 W at 80 °C for 2 h)

Fig. S5. EDX mapping spectra of Act-UST4 (170 kHz, 250 W at 20 °C for 1 h)
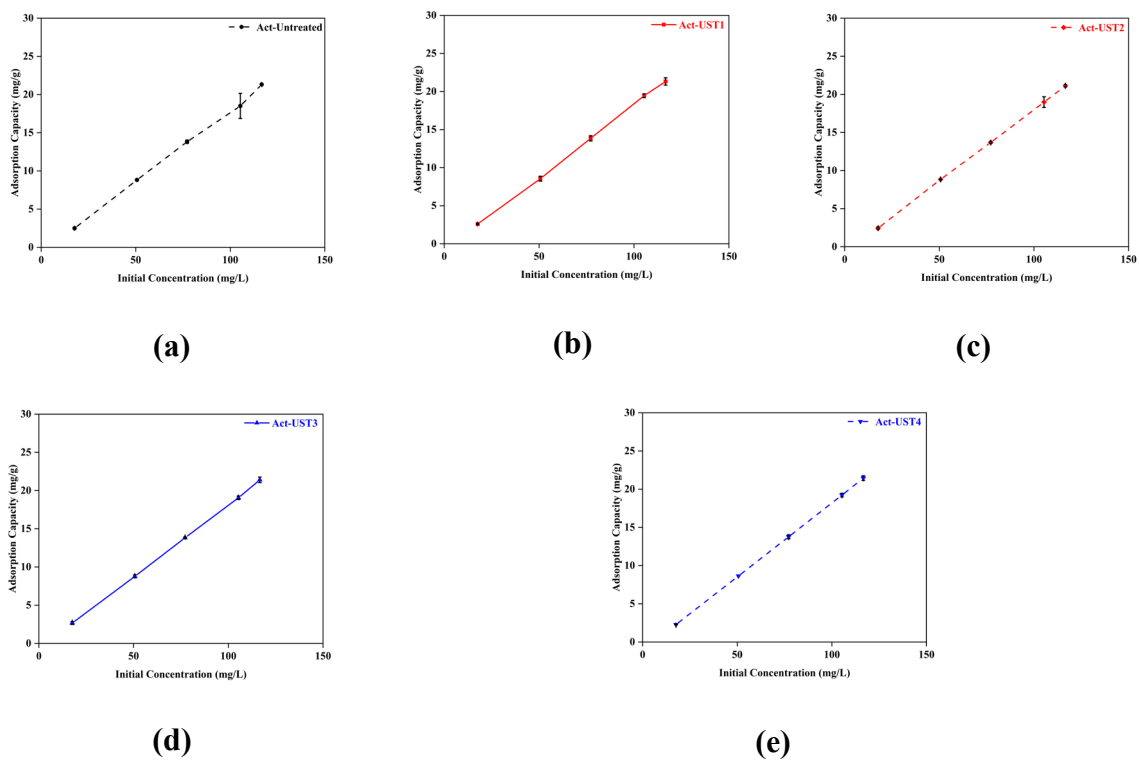

(a)

(b)

(c)

(d)

(e)

Fig. S6. Change in adsorption capacity with initial metal concentration of (a) Act-Untreated
(b) Act-UST1 (40 kHz, 1000 W at 80 °C for 2 h) (c) Act-UST2 (40 kHz, 250 W at 20 °C for 1
h) (d) Act-UST3 (170 kHz, 1000 W at 80 °C for 2 h) and (e) Act-UST4 (170 kHz, 250 W at
20 °C for 1 h)

Table S1. Competitive adsorption behaviour of biochar samples towards Cu (II), Ni (II) and Pb (II) ions.

Metal/Sample	Initial Conc. (mg/L)	Act-Untreated	Act-UST1	Act-UST2	Act-UST3	Act-UST4
Cu (II)	9.06	1.69	1.78	1.79	1.77	1.72
	21.32	4.23	4.12	4.21	4.18	4.1
	42.635	8.27	8.30	7.55	8.06	8.39
	68.135	13.16	13.18	12.52	12.92	13.04
	82.22	15.34	16	16.04	15.37	15.81
Ni (II)	6.24	1.16	1.12	1.23	1.216	1.066
	18.25	3.6	3.49	3.56	3.56	3.43
	33.075	6.34	3.5	5.99	4.95	2.29
	57.885	7.85	4.93	9.44	6.23	3.94
	77.94	6.19	5.04	9.42	3.86	2.24
Pb (II)	9.77	1.79	1.86	1.92	1.89	1.82
	24.64	4.77	4.71	4.74	4.75	4.67
	41.01	6.29	6.31	5.56	6.10	6.40
	33.075	6.31	6.23	5.86	6.11	6.06
	33.68	5.67	6.29	6.35	5.71	5.99